European Journal of Environment and Earth Sciences
www.ej-geo.org

RESEARCH ARTICLE

Ionization Waves, Propagating in Opposite Directions, as in Red Sprites

Dmitry A. Sorokin, Victor F. Tarasenko, Evgenii Kh. Baksht, and Nikita P. Vinogradov

ABSTRACT

The paper is devoted to the study of a pulsed streamer discharge, similar to that in the Earth's upper atmosphere. An experimental setup providing the formation of two ionization waves propagating in opposite directions from a region filled with a plasma formed by the capacitive discharge in low-pressure atmospheric air was created. In a physical experiment, the process of propagation of red ionization waves (streamers) was simulated. It was established that the average propagation velocities of their fronts correspond to those of red sprites. This was shown as a result of spectral studies that at air pressures of 0.4-3 Torr, the radiation color radiation observed visually and captured on an integral photograph from the region of passage of ionization waves is determined by the spectral transitions of the first positive system (FPS) of nitrogen molecules, similar to what occurs for red sprites. In this case, the spectral energy density of radiation in the most intense band of the second positive system (SPS) of the nitrogen molecule with a wavelength of 337.13 nm is an order of magnitude or higher than that in the most intense band of the FPS with the wavelength of 775.32 nm. Using the emission spectra and methods of optical emission spectroscopy (OES), the main parameters of the discharge plasma are estimated. Thus, the created setup makes it possible to simulate the process of the formation of red sprites propagating in opposite directions under laboratory conditions.

Keywords: Ionization Wave, Streamer, Low-Pressure, Red Sprites, Transient Luminous Event.

Published Online: November 20, 2022

ISSN: 2684-446X

DOI: 10.24018/ejgeo.2022.3.6.322

D. A. Sorokin*
Institute of High Current Electronics SB RAS, Tomsk, Russia.
(e-mail: SDmA-70@loi.hcei.tsc.ru)
V. F. Tarasenko
Institute of High Current Electronics SB RAS, Tomsk, Russia.
(e-mail: vft@loi.hcei.tsc.ru)
E. Kh. Baksht
Institute of High Current Electronics SB RAS, Tomsk, Russia.
(e-mail: beh@loi.hcei.tsc.ru)
N. P. Vinogradov
Institute of High Current Electronics SB RAS, Tomsk, Russia.
(e-mail: vinikitavin@mail.ru)

****Corresponding Author***

I. INTRODUCTION

In recent years, much attention has been paid to the study of transient luminous events (TLEs), in particular red sprites, caused by electric discharges occurring in the upper layers of the Earth's atmosphere [1]–[15]. To date, many articles and reviews have been published, which present the results of experimental and theoretical studies of various types of TLEs. Red sprites have been visually seen for a long time. However, these observations have not been documented. They are usually observed over areas of thunderstorm activity. The hypothesis about their existence was first put forward in 1925 [16]. The first color images of these phenomena were published only at the end of the twentieth century [17]. Sprites occur at altitudes of 70–80 km and consist of red colored jets propagating in both towards and away from the Earth's surface [2], [8], [15]. At the altitude of ~50 km from the Earth's surface the color of sprites changes from red to blue [3], [15]. The progress that is currently being observed in the field of TLEs research, in particular red sprites, is due to the use of modern high-resolution devices installed on board aircraft [17] and on the International Space Station [11].

It has been known that the red color of sprites is due to radiation emitted by nitrogen molecules due to spectral transitions of the first positive system (FPS) [1]–[10], [14]. Sprites' propagation velocities and a duration of their radiation pulse have been measured. According to [8], they are (2-5)·10^6 m/s и ~20 ms, respectively. First red sprites usually move down, towards the region of lightning discharges near the Earth's surface, and then up. In this regard, an issue on reasons of the observed sprite propagation process requires additional research.

It is well known, see e.g. [4], [18], [19], that the direction and velocity of propagation of an ionization wave (streamer) depend on the direction of an electric field and its strength E. Red sprites are also formed by large ionization waves (streamers) [1]–[14], [16]. The strength required for the formation of a cathode-directed streamer upon breakdown in a non-uniform electric field is 2-3 times lower than for an anode-directed one [18], [19]. This peculiarity has been confirmed in many studies, including those dealing with low-pressure air.

The purpose of this paper is to develop an experimental setup for the formation and study of red colored ionization waves propagating in opposite directions, corresponding to those occurring in low-pressure regions where red sprites are observed.

II. Experimental Setup and Techniques

Breakdown in long tubes has been studied before [2], [20]–[23]. The difference of this study is that here an electrodeless system is used to initiate ionization waves. A 120-cm-length quartz tube was filled with atmospheric air with a humidity of ≈23%, but first, it was pumped out to a residual pressure of 10^{-2} Torr. The air pressure p in the tube was varied in the range of 0.1-10 Torr. The inner diameter and the wall thickness of the tube were 5 cm and 2.5 mm, respectively. Quartz grade GE 214, from which the tube was made, provided a high transmittance in the ultraviolet (UV) and visible regions of the spectrum. Two annular electrodes were installed in the central part of the tube on its outer surface. The ends of the tubes were mounted with caprolon flanges. One of the electrodes (left, relative to the reader, Fig. 2) was grounded through a current shunt. The second ring was a high-voltage electrode. An interelectrode distance d was 6 cm. To excite the air inside the tube, voltage pulses of positive or negative polarity are formed by a high-frequency generator applied across the electrodes. A voltage pulse amplitude $|U_0|$ could be varied in the range of 1-7 kV. A voltage pulse rise time t_f and its duration τ (FWHM) were ≈350 ns and ≈2 µs, respectively. A pulse repetition rate f was 21 kHz.

In a number of experiments, an additional electrode made of 1-mm-diameter wire was mounted on the left flange, which was either grounded or connected to a constant voltage source. Thus, it was possible to change the electric field between the capacitive discharge plasma between the rings and the left end of the tube. In most experiments, the tube was placed parallel to the surface of the stand and the Earth. This contributed to the convenience of measurements. Installing it perpendicular to the Earth's surface or at other angles did not significantly affect the morphology and characteristics of the discharge.

The voltage U across the gap and the discharge current I_d were measured with an ASA-6039 divider (AKTAKOM) and a hand-made current shunt, respectively. Electric signals from the probes were recorded with an MDO 3104 oscilloscope (Tektronix) with a bandwidth of 1 GHz and a sampling rate of 5 GS/s.

A spectral energy distribution of the discharge plasma in the range of wavelengths Δλ = 190-1100 nm was registered with an HR2000+ES spectrometer (OceanOptics Inc.) with known spectral sensitivity characteristic and an instrumental function $\Delta\lambda_{instr} \approx 0.9$ nm. In addition, to estimate main parameters an emission spectrum of the plasma in Δλ = 300–400 nm was recorded with an HR4000 spectrometer (OceanOptics Inc.) with known spectral sensitivity characteristic and $\Delta\lambda_{instr} \approx 0.2$ nm. Integral images of the discharge plasma glow were captured with a digital camera A100 (Sony). A velocity of ionization waves was determined in experiments with a high-speed photodiode PD025 (Photek) with an LNS20 cathode. It allows to register light pulses in Δλ = 200-900 nm (maximum sensitivity is in Δλ = 200-500 nm) with subnanosecond temporal resolution (~0.8 ns). In this case, the time behavior of a radiation intensity from 4-cm-width regions was recorded. The centers of the regions were located at the distance of 3, 13 and 23 cm from the annular electrode(s). During these measurements, the remaining part of the tube was covered with an opaque screen. Plasma emission spectra were also recorded from these regions.

III. Experimental and Simulation Results

Waveforms of U and I_d are presented in Fig. 1a. In the pressure range Δp = 0.4-9 Torr and at U_0 = 7 kV, the breakdown occurs within the voltage pulse rise time. For the same values of the product of pressure and the gap width pd, the nature of the dependence of the breakdown voltage Ub on pd differed from the Paschen curve. So, in the range Δ(pd) = 54-9 Torr·cm experimental curves $U_b(pd)$ first increase, then they decrease (Fig. 1b). The Paschen curve in this Δ(pd) is monotonically decreasing and U_b is essentially lower (≈6 times for pd = 9 Torr·cm). This circumstance can be explained by the pulsed nature of the supply voltage and the presence of dielectric barriers.

Integral images of the discharge plasma glow at various air pressures are in Fig. 2. An exposure time t_{exp} was 0.2 s. During texp, about 4200 discharges occur in the tube. Thus, each integral image is formed by accumulating individual low-intensity images, which makes it possible to study the dynamics of the development of the discharge at various pressures.

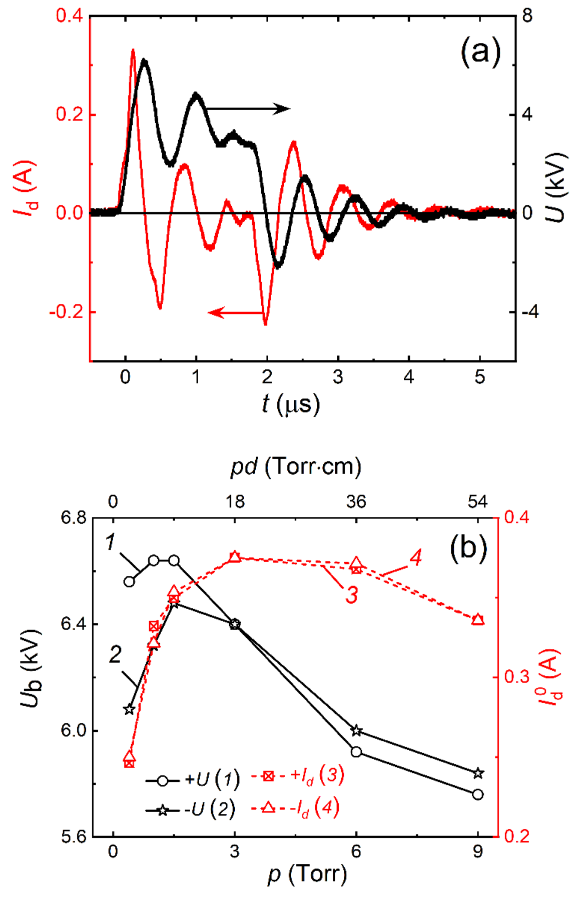

Fig. 1. Waveforms of the voltage U across the gap formed by annular electrodes (black) and discharge current I_d (red) (a). Amplitudes of the breakdown voltage U_b (1, 2) and discharge current I_d^0 (3, 4) at positive (1, 3) and negative (2, 4) polarities of the high-voltage annular electrode (b). p = 1 Torr, $|U_0|$= 7 kV.

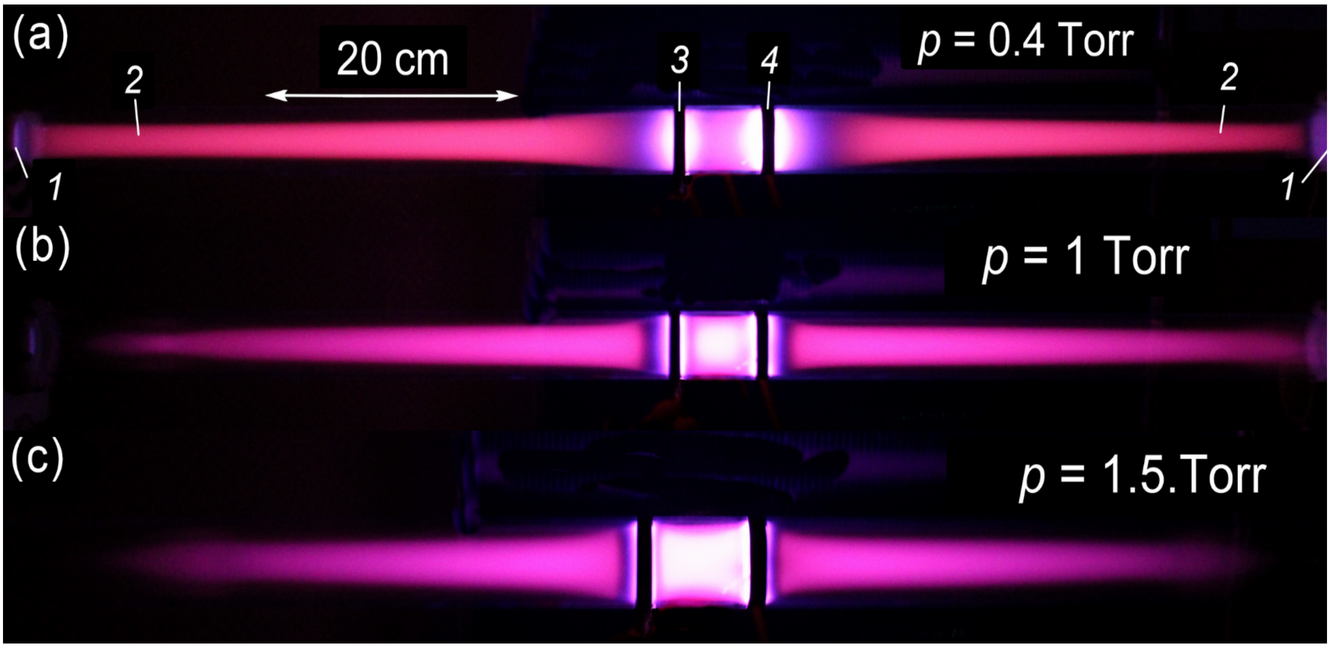

Fig. 2. Integral images of the discharge plasma glow in the tube at air pressures of 0.4 (a), 1 (b) and 1.5 Torr (c). *1* – glow near caprolone flange at the tube end; *2* – ionization waves (streamers); *3*, *4* – grounded and high-voltage annular electrode. U_0 = +7 kV; no additional electrode; t_{exp} = 0.2 s; diaphragm is 5.6.

For this experimental setup the highest E is achieved near the annular electrodes and in the space between them. Therefore, with an increase in p to 6-9 Torr and/or a decrease in $|U_0|$, a diffuse plasma was implemented in the interelectrode region only and no ionization waves observed away from the electrodes.

Decreasing p or increasing $|U_0|$ leads to the propagation of ionization waves from the region occupied by the capacitive discharge plasma in both directions from the annular electrodes. With decreasing air pressure in the tube, the distance over which the ionization waves propagate increased. For $p \leq 1$ Torr it was several dozens of centimeters.

At p in the range of 0.4-3 Torr the glow in the region where the ionization waves propagate is red colored. That is their color corresponds to that of red sprites observed at altitudes of 50-100 km over the Earth's surface [1]–[12], [14], [15].

The additional electrode mounted on the left (Fig. 2, towards the reader) flange, as well as its polarity and potential affect the distance the waves travel. In the case of the grounded additional electrode, the length of the glowing zone from the side of the grounded annular electrode 3 (see Fig. 2) increased and reached the additional electrode with decreasing air pressure. Connecting a constant voltage source to this electrode made it possible to change the length of the ionization wave. In addition, this length depended on the voltage applied across the annular electrodes.

Emission spectra of the plasma were recorded from the interelectrode region, as well as at different distances to the left and to the right from the annular electrodes. Fig. 3 shows a survey emission spectrum in the range of wavelengths of $\Delta\lambda$ = 280-900 nm captured from the ionization wave propagation region. At p = 1 Torr, the largest spectral energy density W_{spec} of the radiation in $\Delta\lambda$ = 280-900 nm is concentrated in vibrational-rotational (V-R) UV bands formed by the second positive system (SPS) of N_2 (Fig. 3a). The band with λ = 337.13 nm has the highest intensity. As the pressure decreased to 0.4 Torr, the distribution of the radiation energy in the spectrum was generally preserved, however, there was a noticeable increase in the intensity of the band with λ = 391.4 nm of the molecular nitrogen ion N_2^+ belonging to the first negative system (FNS). The intensity of the latter could be comparable with that of the band with λ = 391.4 nm of the SPS.

The red colored glow of the discharge plasma observed visually and in photographs is associated with a relatively high radiation energy density contained in the FPS bands at low pressures. The absolute radiation energy density of these bands also increased. The inserted image in Fig. 3a demonstrates the spectral energy distribution in $\Delta\lambda$ = 500-900 nm, where radiation is formed predominantly by spectral transitions of the first positive system (FPS) of a nitrogen molecule N_2.

Ratios P_{337}/P_{775} of the intensities of the radiation of the most intense bands in the SPS and FPS, respectively, at various distances L from the outer edge of the grounded annular electrode are shown in Fig. 3b. Despite the fact that this ratio increases by a factor of 5 with increasing pressure from 0.4 to 9 Torr, the red component dominates in the color of the plasma glow.

Using better resolved spectra in $\Delta\lambda$ = 300-400 nm recorded with the HR4000 spectrometer equipped with a fiber optic cable (Fig. 4a) and methods of the optical emission spectroscopy (OES) [24]–[28] time averaged main plasma parameters were estimated. This procedure was performed for the discharge in the tube filled with air at p = 1 Torr. The plasma parameters were determined for the interelectrode region, as well as at L = 3, 13 and 23 cm from the annular electrodes.

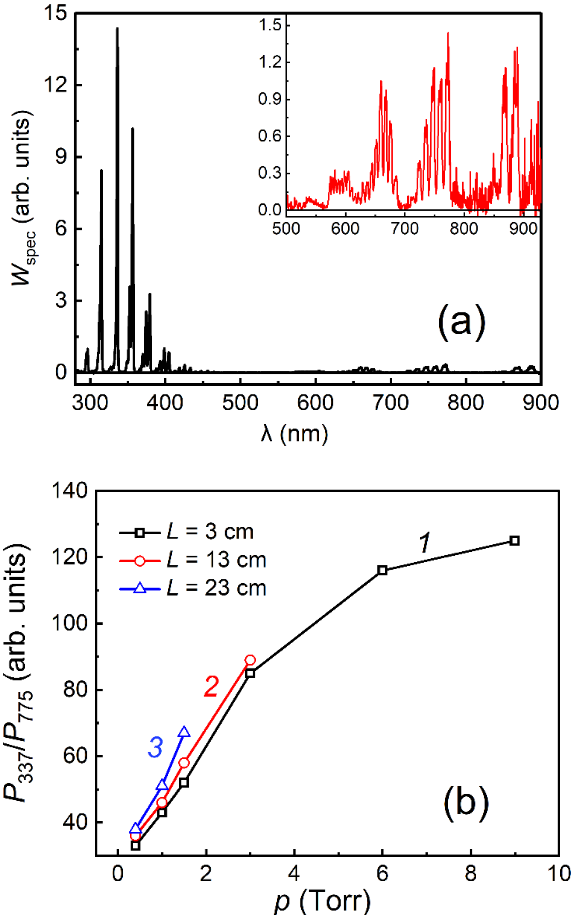

Fig. 3. Emission spectra of the discharge plasma in Δλ = 280-900 nm at p = 1 Torr (a). The spectrum in Δλ = 500-900 nm (inserted image) was recorded with a filter with absorption in the spectral range shorter than 500 nm. Ratios of the radiation intensities of the most intense bands in the SPS (λ = 337.13 nm) and FPS (λ = 775.32 nm), respectively, at various distances L = 3 (*1*), 13 (*2*) and 23 cm (*3*) from the grounded annular electrode (b).

Using better resolved spectra in Δλ = 300-400 nm recorded with the HR4000 spectrometer equipped with a fiber optic cable (Fig. 4a) and methods of the optical emission spectroscopy (OES) [24]–[28] time averaged main plasma parameters were estimated. This procedure was performed for the discharge in the tube filled with air at p = 1 Torr. The plasma parameters were determined for the interelectrode region, as well as at L = 3, 13 and 23 cm from the annular electrodes.

Applying the Boltzmann method [27], [28] to the SPS bands (spectral regions 1, 2 and 3 in Fig. 4a) rotational T_{rot} and vibrational T_{vib} temperatures were determined. Their values are, correspondingly, T_{rot} = 340-360 K и T_{vib} = 2700 K. The larger value of T_{rot} corresponds to the interelectrode space. As for T_{vib}, this value remains practically unchanged over the entire length of the discharge tube. Using the known ratio $T_g = 1.09 \cdot T_{rot}$, the temperature of heavy particles T_g in the discharge plasma was determined. This temperature is in the range of 370-390 K.

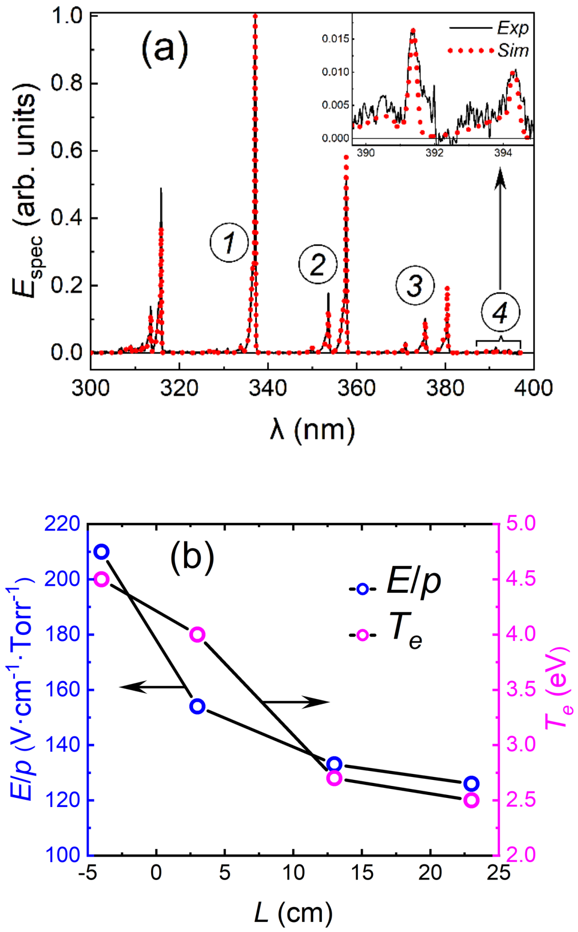

Fig. 4. Experimental (*Exp*, solid) and obtained in simulation (*Sim*, dotted) spectral energy distribution in Δλ = 300-400 nm of the radiation of the capacitive discharge plasma between electrodes. *1* – V-R band of the SPS with λ = 337.13 nm used for determination T_{rot} and T_g; *2*, *3* – sequences of V-R bands of the SPS in Δλ = 350-360 nm and Δλ = 370-380 nm used for determination T_{vib}; *4* – spectral range containing V-R bands of the FNS (λ = 391.4 nm) and SPS (λ = 394.3 nm) used for determination T_e and E/p: a) T_e and E/p at various distances L from the grounded annular electrode; b) The point L = -4 cm corresponds the center between the annular electrodes. p = 1 Torr.

The spectral region 4 (see Fig. 4a) containing radiation bands of a molecular ion N_2^+ (391.4 nm, FNS) and molecule N_2 (394.3 nm, SPS) of nitrogen, as well as method based on the determination of peak intensities of these bands [24]–[26] made it possible to estimate electron temperature T_e and reduced electric field strength E/p (initially E/N, where N is gas concentration). Fig. 4b demonstrates how these plasma parameters change with the distance from the interelectrode region (the point L = -4 cm is the interelectrode region). In this case, there was no additional electrode at the tube's end. It is seen that the highest T_e and E/p values are achieved in the space between annular electrodes and then they decrease with increasing L. Despite this, their absolute values remain quite high. This fact confirms the assumption that the glow regions directed to both sides from the annular electrodes are the result of the propagation of ionization waves. This version of the formation of the discharge is also supported by the shape of the plasma emission spectra in different regions at p = 0.4 Torr. In this case, the intensity of the molecular ion band at 391.4 nm exceeds that of the molecule band at 394.3 nm over the entire length of the tube, i.e. under these conditions, much larger T_e and E/p values take place.

It should be noted that the correctness of the estimation of the above values of the plasma parameters is confirmed by the results of modeling the plasma emission spectrum in this wavelength range using the SPECAIR code [29] – the calculated curve *Sim* (points) very accurately describes the experimental curve *Exp* (solid) when using the values of temperatures obtained from the experimental data.

For clarity, the plasma emission spectrum in Fig. 4a is presented for the interelectrode region only. With L, the shape of the spectrum does not change as a whole, only the ratio of the peak intensities of the nitrogen ion (391.4 nm) and molecule (394.3 nm) bands changes, which, taking into account the values of such parameters as T_e and E/N, is fully described.

It should also be noted that when modeling the emission spectra, it was also possible to estimate the electron density N_e. In this case, a curious fact is that as the distance from the interelectrode zone increases, its value increases from ~$4\cdot10^{11}$ to ~$2\cdot10^{12}$ cm^{-3}. This, in turn, can be explained by the fact that with increasing L, the diameter of the ionization wave, which is the area of the current flow zone, decreases at a constant value of the flowing current.

IV. Discussion

Let's analyze the obtained results and compare them with the known data on the development of red sprites. In our experiments, the formation of ionization waves propagating to opposite directions from the capacitive discharge region was observed. For the formation of red sprites, it is also necessary that the concentration of electrons and ions in the plasma be sufficiently high. It can be assumed that diffuse discharges between regions of noctilucent clouds with charges of different polarity are the source of dense plasma. It is known that noctilucent clouds, consisting of ice crystals, form approximately at the same altitudes as red sprites [30]. The separation of charges in them occurs similar to how this process occurs in thunderclouds near the surface of the Earth [16], [31]. In the case of low-pressure diffuse discharges at high altitudes, the plasma glow is quite weak. Therefore, their radiation has not yet been experimentally registered. Nevertheless, we believe that such discharges near notilucent clouds initiate, with sufficient E/N, the formation of ionization waves – sprites. In should be noted that in some cases, at high altitudes, sprites are initiated by micrometeors [32], [33]. At the initial stages, the direction of downward movement of sprites is set by E, which should be directed from the place where a sprite appears to a negatively charged surface. Such a surface can be the upper part of thunderclouds. Although the upper layer of thunderclouds is usually positively charged [2], [4], [19], [31], positive lightning carries the Earth's negative charge into this region. As follows from the experiments on the created setup, the length of the left ionization wave (propagating from the grounded ring) increases when negative voltage is applied to the additional electrode or when it is grounded. When forming downward sprites, their length can be limited either by decreasing E or by increasing p. First, downward sprites propagate into a denser medium. In addition, the electric field strength above thunderclouds changes due to the presence of lightning and the sprite development.

Apparently, a change in E affects the direction and length of the propagation of upward red sprites [2], [5], [6] Thus, the chaotic direction of sprite propagation observed at altitudes of about 70 km can be explained by the uneven distribution of charges in the region of noctilucent clouds.

During the formation of sprites, the primary direction of their movement towards the Earth is determined by the electric field of the negative charge, which is concentrated in the upper part of the clouds during lightning. At the next stage, this field decreases, and sprites are formed, which move up to the layer of excess negative charge. This can lead to a delay in the appearance of upward-facing sprites.

V. Conclusion

Thus, we report on the creation of a setup that allows to the formation, at low pressures of atmospheric air, two ionization waves propagating in opposite directions and to measure their propagation velocities. It has been established that the velocity of the front of ionization waves (streamers) corresponds to the average velocity of propagation of red sprites. As with sprites, this velocity decreases as these waves propagate. Thus, at $p = 1.5$ Torr at distances of 13 and 23 cm from the ring grounded electrode, its value was 0.17 and 0.12 cm/ns, respectively. It has been shown that under the given conditions of formation of ionization waves in $\Delta p = 0.4$-3 Torr, their color is determined by the radiation of the FPS and corresponds to the radiation color of red sprites. At the same time, the radiation spectral energy density concentrated in the bands of the SPS and FNS of nitrogen in the region of a high electric field between the annular electrodes, is an order of magnitude or higher than that concentrated in the bands of the FPS. Thus, this setup makes it possible to simulate the conditions and the process of formation of red sprites in a laboratory.

Acknowledgment

The authors are thankful to G.V. Naidis for the helpful discussion and to D.S. Pechenitsin for the development and creation of the voltage pulse generator with a high pulse repetition rate.

Funding

The study is funded by the Ministry of Science and Higher Education of the Russian Federation within Agreement no. 075-15-2021-1026 of November 15, 2021.

Conflict of Interest

Authors declare that they do not have any conflict of interest.

References

[1] Rodger CJ. Red Sprites, Upward lightning, and VLF perturbations. *Rev. Geophys.* 1999 Aug 01; 37(3):317–336. doi:10.1029/1999RG900006.

[2] Williams ER. Sprites, elves, and glow discharge tubes. Phys. Today. 2001 Nov; 54(11):41–47. doi:10.1063/1.1428435.

[3] Füllekrug M, Mareev EA, and Rycroft MJ (editors). *Sprites, Elves and Intense Lightning Discharges*. Dordrecht: Springer; 2006.
[4] Pasko VP. Red sprite discharges in the atmosphere at high altitude: the molecular physics and the similarity with laboratory discharges. *Plasma Sources Sci. Technol.* 2007 Jan 31; 16(1):S13. doi:10.1088/0963-0252/16/1/S02.
[5] Kanmae T, Stenbaek-Nielsen HC, McHarg MG. Altitude resolved sprite spectra with 3 ms temporal resolution. *Geophys. Res. Lett.* 2007 Apr 13; 34(7):L07810. doi10.1029/2006GL028608.
[6] Stenbaek-Nielsen HC, McHarg MG. High time-resolution sprite imaging: observations and implications. *J. Phys. D: Appl. Phys.* 2008 Nov 20; 41(23):234009. doi:10.1088/0022-3727/41/23/234009
[7] Raizer YP, Milikh GM, Shneider MN. Streamer- and leader-like processes in the upper atmosphere: models of red sprites and blue jets. *JGR: Space Physics.* 2010 Jul 07; 115(A7):A00E42. doi:10.1029/2009JA014645.
[8] Kanmae T, Stenbaek-Nielsen HC, McHarg MG, Haaland RK. Diameter-speed relation of sprite streamers. *J. Phys. D: Appl. Phys*. 2012 Jun 22;45(27):275203. doi:10.1088/0022-3727/45/27/275203.
[9] Gordillo-Va´zquez FJ, Luque A, Simek M. Near infrared and ultraviolet spectra of TLEs. *JGR: Space Physics.* 2012 May 26; 117(A5):A05329. doi10.1029/2012JA017516.
[10] Qin J, Celestin S, Pasko VP. Formation of single and double-headed streamers in sprite-halo events. *Geophys. Res. Lett.* 2012 Mar 15; 39(5):L05810. doi:10.1029/2012GL051088.
[11] Neubert T, Østgaard N, Reglero V, Blanc E, Chanrion O, Oxborrow CA, *et al.* The ASIM mission on the International Space Station. *Space Sci. Rev*. 2019 Mar 12; 215(26):1–17. doi:10.1007/s11214-019-0592-z.
[12] Wang Y, Lu G, Ma M, Zhang H, Fan Y, Liu G, *et al.* Triangulation of red sprites observed above a mesoscale convective system in North China. *Earth and Planetary Physics.* 2019 Mar 25; 3(2):111–125. doi:10.26464/epp2019015.
[13] Jiang F, Huang C, Wang Y. Emission spectrum of sprites caused by the quasi-electrostatic field above thunderstorm clouds. *Meteorology and Atmospheric Physics*. 2019 Jan 24; 131(3):421–430. doi:10.1007/s00703-018-0579-4.
[14] Kuo CL, Williams E, Adachi T, Ihaddadene K, Celestin S, Takahashi Y, *et al.* Experimental validation of N_2 emission ratios in altitude profiles of observed sprites. *Frontiers in Earth Science.* 2021 Nov 16; 9:1102–1114. doi:10.3389/feart.2021.687989.
[15] Facebook.com. [Internet]. 2021 [cited 2021 January 01]. Available from: http://www.facebook.com/frankie.lucena.1.
[16] Wilson CTR. The electric field of a thundercloud and some of its effects. *Proc. Phys. Soc. London.* 1924 Jan; 37(1):32D. doi:10.1088/1478-7814/37/1/314.
[17] Sentman DD, Wescott EM, Osborne DL, Hampton DL, Heavner MJ. Preliminary Results from the Sprites94 Aircraft Campaign: 1. Red Sprites. Geophys. Res. Lett. (1995) 22(10): 1205–08. doi:10.1029/95GL00583
[18] Raizer YP, Allen JE. *Gas discharge physics*. Berlin: Springer; 1991.
[19] Ebert U, Nijdam S, Li C, Luque A, Briels T, van Veldhuizen E. Review of recent results on streamer discharges and discussion of their relevance for sprites and lightning. *JGR: Space Physics.* 2010 Jul 10; 115(A7):A00E43. doi:10.1029/2009JA014867.
[20] Vasilyak LM, Kostyuchenko SV, Kudryavtsev NN, Filyugin IV. Fast ionisation waves under electrical breakdown conditions. *Phys. Usp.* 1994 Mar; 37(3):247–268. doi:10.1070/PU1994v037n03ABEH000011.
[21] Williams E, Valente M, Gerken E, Golka R. Sprites, calibrated radiance measurements with an air-filled glow discharge tube: application to sprites in mesosphere. In: Sprites, *Elves and Intense Lightning Discharges*. Füllekrug M, Mareev EA, and Rycroft MJ EDS. Dordrecht: Springer, 2006. pp. 237–251.
[22] Anikin NB, Zavialova NA, Starikovskaia SM, Starikovskii AY. Nanosecond-discharge development in long tubes. *IEEE Trans. Plasma Sci.* 2008 Jan 29; 36:902–903. doi:10.1109/TPS.2008.924504.
[23] Sosnin EA, Babaeva NYu, Kozyrev AV, Kozhevnikov VYu, Naidis GV, Skakun VS, Panarin VA, Tarasenko VF. Modeling of transient luminous events in earth's middle stmosphere with apokamp discharge. *Phys. Usp.* 2021 Feb; 64:191–210. doi:10.3367/UFNe.2020.03.038735.
[24] Nassar H, Pellerin S, Musiol K, Martinie O, Pellerin N, Cormier J-M. N2+/N2 ratio and temperature measurements based on the first negative N_2^+ and second positive N_2 overlapped molecular emission spectra. *J. Phys. D: Appl. Phys.* 2004 Jun 30; 37(14):1904–1916. doi:10.1088/0022-3727/37/14/005.
[25] Britun N, Gaillard M, Ricard A, Kim YM, Kim KS, Han JG. Determination of the vibrational, rotational and electron temperatures in N_2 and Ar–N_2 rf discharge. *J. Phys. D: Appl. Phys.* 2007 Feb 02; 40(4):1022–1029. doi:10.1088/0022-3727/40/4/016.
[26] Paris P, Aints M, Valk F, Plank T, Haljaste A, Kozlov KV, Wagner H-E. Intensity ratio of spectral bands of nitrogen as a measure of electric field strength in plasmas. *J. Phys. D: Appl. Phys.* 2005 Oct 2005; 38(21):3894–3899. doi:10.1088/0022-3727/38/21/010.
[27] Ochkin VN. *Spectroscopy of low temperature plasma*. Weinheim: Wiley VCH Verlag GmbH & Co.; 2009.
[28] Philips DM. Determination of gas temperature from unresolved bands in the spectrum from a nitrogen discharge. *J. Phys. D: Appl. Phys.* 1975 Mar; 9(3):507–521. doi:10.1088/0022-3727/9/3/017.
[29] Laux CO. Radiation and Nonequilibrium Collisional-Radiative Models. In: *Physico-Chemical of High Enthalpy and Plasma Flows*. von Karman Institute Lecture Series 2002-2007. Fletcher D, Carbonnier J-M, Sarma GSR, Magin T. Eds. Belgium: Rhode Saint Genèse, 2002.
[30] Hervig M, Thompson RE, McHugh M, Gordley LL, Russell III JM, Summers ME. First confirmation that water ice is the primary component of polar mesospheric clouds. *Geophys. Res. Lett.* 2001 Mar 15; 28(6):971–974. doi:10.1029/2000GL012104.
[31] Bazelyan EM, Raizer YP. *Lightning physics and lightning protection*. Boca Raton: CRC Press; 2000.
[32] Janalizadeh R, Pasko VP. Sprite streamer initiation from species deposited in the trail of overdense meteors under the application of lightning-induced electric field and emissions (*Abstarct #AE21A-08*, *AGU Fall Meeting*); 2018 Dec 14–18, Washington D.C., USA.
[33] Tarasenko V, Vinogradov N, Beloplotov D, Burachenko A, Lomaev M, Sorokin D. Influence of nanoparticles and metal vapors on the color of laboratory and atmospheric discharges. *Nanomaterials.* 2022 Feb 15; 12:652. doi:10.3390/nano12040652.

Dmitry A. Sorokin received the Ph.D. degree from the Physics Department, National Research Tomsk State University, Tomsk, Russia, in 2009. He is currently the Head of the Laboratory of Optical Radiations, Institute of High Current Electronics, Siberian Branch, Russian Academy of Sciences (IHCE SB RAS), Tomsk. In 2015, he defended his Ph.D. thesis. He has authored or coauthored over 80 publications. Research interests: physics of a gas discharge, optics, physics of low-temperature plasma, and spectroscopy of low-temperature plasma. He made a contribution to the field of studies of high-voltage nanosecond discharges initiated by runaway electrons: the electrical properties of such discharges, the properties and parameters of the plasma, and the properties of runaway electron beams.

Victor F. Tarasenko was received the Ph.D. in 1976, the D.Sc. in 1988, and the Professor in 1994. Currently, he is a Chief Researcher of Optical Radiation Laboratory Institute of High Current Electronics SB RAS and the Professor of Tomsk State University and Tomsk Polytechnic University, Russia. V.F. Tarasenko co-authored more than 900 publications, 80 inventions, 23 reviews, 11 monographs, and 3 textbooks for students. The name of the V.F. Tarasenko is included in the database of the best scientists in the world, compiled by representatives of Stanford University based on citation rates and the number of published works (2020). His research interests are in physics of gas discharges and generation of runaway electrons, dense-gas pulsed lasers, spontaneous UV and VUV sources (excilamps).

Evgenii Kh. Baksht received the M.S. degree in optoelectronic devices and systems from Tomsk State University, Tomsk, Russia, in 1979 and Ph.D. degree in electrophysics from the Institute of High Current Electronics (IHCE), Tomsk, Russia, in 2003. Since 1980, he is currently a Senior Researcher at the Laboratory of Optical Radiation of IHCE. He has co-authored over 170 publications His current research interests include the gas discharge sources of spontaneous and stimulated emission radiation, the physics of nanosecond high-voltage gas discharges and generation of runaway electrons.

European Journal of Environment and Earth Sciences
www.ej-geo.org

Nikita P. Vinogradov received the M.S. degree in power industry and electrical engineering from Tomsk Polytechnic University, Tomsk, Russia, in 1920. He is currently a Graduate Student at the Laboratory of Optical Radiation of IHCE. He has co-authored 4 publications His current research interests the physics of nanosecond high-voltage gas discharges and generation of runaway electrons.